Crystal Structure and Spectroscopic and Magnetic Properties of Two *cis*-Azido Catenas of Nickel(II): *cis-catena*-(μ-N_3)[Ni(bipy)$_2$](X) (X = ClO_4, PF_6)

Roberto Cortés,† Karmele Urtiaga,‡ Luis Lezama,† J. Luis Pizarro,‡ Aintzane Goñi,† M. Isabel Arriortua,‡ and Teófilo Rojo*,†

Departamentos de Química Inorgánica y Mineralogía-Petrología, Universidad del País Vasco, Aptdo. 644, 48080 Bilbao, Spain

Received February 23, 1994®

The compounds *cis-catena*-(μ-N_3)[Ni(bipy)$_2$](ClO_4) (**1**) and *cis-catena*-(μ-N_3)[Ni(bipy)$_2$](PF_6) (**2**) (where bipy = 2,2′-bipyridine) have been synthesized and characterized. Both crystallize in the monoclinic $P2_1/c$ space group. For **1**, a = 20.830(3) Å, b = 15.497(4) Å, c = 13.90(1) Å, β = 101.72(3)°, V = 4393(3) Å^3, Z = 4, R = 0.065, and R_w = 0.070. In the case of compound **2**, a = 21.173(3) Å, b = 15.781(2) Å, c = 13.930(4) Å, β = 100.04(2)°, V = 4583(2) Å^3, Z = 4, R = 0.071, and R_w = 0.075. The nickel(II) ions are octahedral with the two bipy ligands and end-to-end azido bridges in a *cis*-arrangement. This configuration of the azido bridges has not been reported so far. Magnetic measurements of both compounds show strong antiferromagnetic couplings between the nickel cations through the azido ions. The obtained exchange parameters are J = –33.0 cm^{-1} for the perchlorate compound **1** and J = –22.4 cm^{-1} for the hexafluorophosphate complex **2**, with a gyromagnetic tensor value of g = 2.15 in both cases. The magnetic behavior has been compared with that of the *trans*-azido chains known in the literature and analyzed by extended Hückel MO calculations.

Introduction

Dinuclear nickel(II) systems with end-to-end pseudohalide bridges were studied some years ago.[1-3] However, compounds having either end-on pseudohalide bridges or 1D polynuclear systems with pseudohalide-bridges were not explored in Ni(II) chemistry. In the last few years our group have developed a synthetic strategy to obtain compounds of this unknown type. We successfully obtained and fully characterized the first end-on-pseudohalide bridged Ni(II) systems with cyanato and azido ligands.[4-6] An interesting characteristic of these latter compounds, observed in related dinuclear Ni(II) systems,[7,8] is that contrary to the antiferromagnetic behavior observed in the end-to-end azido bridges, the end-on azido ones show ferromagnetic interactions.

The polydentate ligands (generally tridentate aromatic amine ligands) used to form these kinds of compounds gave rise to a *cis* coordination of the bridging groups around the nickel(II) ion, which favors the obtaining of dinuclear complexes. The rigidity effect of the tridentate ligand observed in the copper(II) compounds to obtain polynuclear systems[9,10] is now being investigated in nickel(II) systems. As a result, the use of nonrigid tridentate alifatic amine ligands has lead to a nickel(II) chain structure.[11] Recently, the first nickel(II) chain containing a tetradentate amino ligand and a single azido bridge, in *trans* conformation, has been reported.[12] However, as far as we are aware no nickel(II)–azido chains with *cis* conformation are known.

Taking into account all these facts, the aim of this paper was to obtain nickel(II) chains with the unknown *cis* arrangement. To favor such a position around the metal ion, we decided to use two bidentate aromatic amine ligands, in this case 2,2′-bipyridine (bipy), to block the metal. The reason for this choice is that the known complexes of the nickel(II) ion with the bipy ligand in 1:2 proportion show the wanted *cis* position, therefore minimizing the steric crowding caused by the rigidity and size of the ligand.[13-15] As a consequence, the complexes [Ni(bipy)$_2$(N_3)](ClO_4) (**1**) and [Ni(bipy)$_2$(N_3)](PF_6) (**2**) have been prepared and characterized. Both constitute the first nickel(II) chain-structures with end-to-end azido bridges having a *cis* arrangement. Magnetic measurements for both compounds **1** and **2** indicate a strong antiferromagnetic coupling between the nickel(II) ions.

Experimental Section

Materials. 2,2′-Bipyridine (Aldrich), nickel chloride (Aldrich), sodium perchlorate (Sigma), potassium hexafluorophosphate (Fluka), and sodium azide (Fluka) were purchased and used without further purification.

Synthesis. ***Caution!*** Perchlorate salts of metal complexes with organic ligands are potentially explosive. Only a small amount of material should be prepared, and it should be handled with caution.

Synthesis of [Ni(bipy)$_2$(N_3)]Y (Y= ClO_4 (1) and PF_6 (2)). Both compounds were obtained by treating aqueous solutions (20 mL) containing 1 mmol of the compound [Ni(bipy)$_2$(N_3)$_2$]·H_2O (previously prepared by reacting [Ni(bipy)$_2$$Cl_2$]·2$H_2O$ and sodium azide) with an excess of sodium perchlorate or potassium hexafluorophosphate to obtain compounds **1** and **2** respectively. The samples were stirred while being moderately heated for 1 h. The resulting solution was left standing at

† Departamento de Química Inorgánica, Universidad del País Vasco.
‡ Departamento de Mineralogía-Petrología, Universidad del País Vasco.
® Abstract published in *Advance ACS Abstracts,* August 1, 1994.

(1) Pierpont, C. G.; Hendrickson, D. N.; Duggan, D. M.; Wagner, F.; Barefield, E. K. *Inorg. Chem.* **1975**, *14*, 604.
(2) Duggan, D. M.; Hendrickson, D. N. *Inorg. Chem.* **1973**, *22*, 2422.
(3) Chaudhuri, P.; Guttmann, M.; Ventur, D.; Wieghardt, K.; Nuber, B.; Weiss, J. *J. Chem. Soc., Chem. Commun.* **1985**, 1618.
(4) Arriortua, M. I.; Cortés, R.; Mesa, J. L.; Lezama, L.; Rojo, T.; Villeneuve, G. *Transition Met. Chem. (Weinheim, Ger.)* **1988**, *13*, 371.
(5) Arriortua, M. I.; Cortés, R.; Lezama, L.; Rojo, T.; Solans, X.; Font-Bardia, M. *Inorg. Chim. Acta* **1990**, 174, 263.
(6) Cortés, R.; Larramendi, J. I. R.; Lezama, L.; Rojo, T.; Urtiaga, M. K.; Arriortua, M. I. *J. Chem. Soc., Dalton Trans.* **1992**, 2723.
(7) Escuer, A.; Vicente, R.; Ribas, J. *J. Magn. Magn. Mater.* **1992**, *110*, 181.
(8) Vicente, R.; Escuer, A.; Ribas, J.; Salah el Fallah, M.; Solans, X.; Font-Bardia, M. *Inorg. Chem.* **1993**, *32*, 1920.
(9) Rojo, T.; Mesa, J. L.; Arriortua, M. I.; Savariault, D.; Galy, J.; Villeneuve, G.; Beltrán, D. *Inorg. Chem.* **1988**, *27*, 3904.
(10) Rojo, T.; Cortés, R.; Larramendi, J. I. R.; Madariaga, G. *J. Chem. Soc., Dalton Trans.* **1992**, 2125.
(11) Vicente, R.; Escuer, A.; Ribas, J.; Solans, X. *Inorg. Chem.* **1992**, *31*, 1276.
(12) Escuer, A.; Vicente, R.; Ribas, J.; Salah El Fallah, M.; Solans, X. *Inorg. Chem.* **1993**, *32*, 1033.
(13) Osakada, K.; Yamamoto, A. *Acta Crystallogr.* **1984**, *C40*, 85.
(14) Hao, S.; Jiang, Z.; Liao, D.; Zhang, Z.; Wang, G. *Gaodeng Xuexiao Huaxue Xuebao* **1991**, *12*, 427.
(15) Urtiaga, M. K.; Pizarro, J. L.; Cortés, R.; Larramendi, J. I. R.; Goñi, A. *Acta Crystallogr.* **1984**, *C50*, 56.

0020-1669/94/1333-4009$04.50/0

Table 1. Summary of Crystallographic Data and Parameters for $[Ni(bipy)_2(N_3)](ClO_4)$ (**1**) and $[Ni(bipy)_2(N_3)](PF_6)$ (**2**)

	1	**2**
formula	$C_{40}H_{32}N_{14}O_8Cl_2Ni_2$	$C_{40}H_{32}N_{14}Ni_2F_{12}P_2$
fw	1025.11	1116.12
cryst syst	monoclinic	monoclinic
space group	$P2_1/c$ (No. 14)	$P2_1/c$ (No. 14)
a, Å	20.830(3)	21.173(3)
b, Å	15.497(4)	15.781(2)
c, Å	13.90(1)	13.930(4)
β, deg	101.72(3)	100.04(2)
V, Å^3	4393(3)	4583(2)
Z	4	4
T, °C	25	25
λ, Å	0.710 69	0.710 69
ρ_{obs}, g cm^{-3}	1.54(3)	1.60(3)
ρ_{calc}, g cm^{-3}	1.55	1.617
μ, cm^{-1}	10.49	9.88
R^a	0.065	0.071
$R_w{}^b$	0.070	0.075

^{a} $R = [\Sigma(|F_o| - |F_c|)/\Sigma|F_o|]$. ^{b} $R_w = [\Sigma w(|F_o| - |F_c|)^2/\Sigma w|F_o|^2]^{1/2}$.

room temperature to obtain, after several days, good quality needle-prisms of both compounds adequate for the X-ray diffraction study.

Both compounds were satisfactorily analized for C, H, N with the formula $C_{20}H_{16}N_7O_4ClNi$ and $C_{20}H_{16}N_7NiF_6P$ for **1** and **2**, respectively.

Physical Measurements. IR spectra were recorded on a Nicolet 520 FTIR spectrophotometer in the 4000–400-cm^{-1} region. Reflectance spectra were obtained with a Perkin Elmer UV–visible spectrometer. Magnetic measurements were carried out on a polycrystalline sample with a pendulum type susceptometer/magnetometer (Manics DSM8) equipped with a helium continuous flow cryostat working in the 4.2–300 K range. The magnetic field was approximately 10 000 G. Diamagnetic corrections were estimated from Pascal tables.

X-ray Structural Determinations. Diffraction data for **1** and **2** were collected at room temperature on an Enraf-Nonius CAD4 automated diffractometer using graphite-monochromated Mo Kα radiation (λ = 0.710 69 Å). Details on crystal data, intensity collection, and some features of the structure refinement for both compounds are reported in Table 1. Lattice constants were obtained by a least-squares fit of 25 reflections in the range $8° < \theta < 12°$. The intensities of three standard reflections were measured every 2 h and showed no significant decrease in intensity.

For the compound **1**, 11712 reflections were measured in the range $1 \le \theta \le 28°$. A total of 4115 reflections are assumed to have been observed, applying the criterion $I \ge 2.5\sigma(I)$. For the compound **2**, 14362 reflections were measured in the range $1 \le \theta \le 30°$, 4528 of which are considered to have been observed, applying the condition $I \ge 2.5\sigma(I)$. Correction for Lorentz and polarization effects were done, but not for absorption. Direct methods (MULTAN)[16] were employed to solve both structures. They were then refined by the full-matrix least-squares method, using the SHELX76[17] computer program. The function minimized was $\sum w[|F_o| - |F_c|]^2$, where $w = (\sigma^2|F_o| + p|F_o|^2)^{-1}$ [p values 0.00146 (**1**) and 0.0004 (**2**)]. The scattering factors were taken from ref 18. All non-hydrogen atoms were assigned anisotropic thermal parameters. H positions were not calculated. The final R factors were R = 0.065 (R_w = 0.070) for compound **1** and R = 0.071 (R_w = 0.075) for compound **2**. Maximum and minimum peaks in final difference synthesis were 0.76 and –0.46 e Å^{-3}, and 0.64 and –1.22 e Å^{-3} for compounds **1** and **2**, respectively. The final atomic positional parameters for the non-hydrogen atoms of **1** and **2** are listed in Tables 2 and 3, respectively.

Results and Discussion

Description of the Structures of $[Ni(bipy)_2(N_3)]Y$ (Y = ClO_4 (1), PF_6 (2)). The structures of both compounds consist of cationic units formulated by $[Ni(bipy)_2(N_3)]_2^{2+}$ and ClO_4^- (**1**) and PF_6^- (**2**) counterions. The cationic units are bridged by azide ligand in an end-to-end fashion to form 1D chain structures $[Ni(bipy)_2(N_3)]_n^{n+}$ that are isolated by the counterions sited in the interchain spaces. In both cases, the asymmetric unit is formed by two of these entities that are attached consecutively in a chain (Figure 1). Different perspective views of the chains are shown in Figure 2. The selected bond distances and angles are given in Table 4. The nickel(II) ions are coordinated by the four nitrogen atoms of the two bipy ligands [NiA–N1A, –N2A, –N3A, –N4A: 2.065-

Table 2. Fractional Atomic Coordinates and Equivalent Thermal Parameters for $\{[Ni(bipy)_2N_3](ClO_4)\}_2$ (**1**)

atom	x	y	z	B_{eq},^{a} Å^3
NiA	0.20784(4)	0.43611(6)	0.69430(6)	4.18(2)
N1A	0.2957(3)	0.4700(4)	0.7843(4)	4.90(18)
N2A	0.1758(3)	0.5070(4)	0.8031(4)	4.88(17)
N3A	0.2011(3)	0.5414(4)	0.5988(4)	4.45(16)
N4A	0.1186(3)	0.4143(4)	0.6023(4)	4.66(17)
N5A	0.2045(3)	0.3258(4)	0.7791(4)	5.25(19)
N6A	0.2501(3)	0.2808(4)	0.8074(4)	4.17(16)
N7A	0.2963(3)	0.2386(4)	0.8380(4)	5.04(19)
C1A	0.3555(4)	0.4437(6)	0.7709(6)	6.32(29)
C2A	0.4128(4)	0.4745(7)	0.8320(7)	7.32(35)
C3A	0.4088(5)	0.5310(7)	0.9091(8)	7.57(32)
C4A	0.3465(5)	0.5557(6)	0.9239(6)	6.47(30)
C5A	0.2914(4)	0.5234(5)	0.8606(5)	4.79(22)
C6A	0.2252(4)	0.5410(4)	0.8724(5)	4.93(22)
C7A	0.2110(5)	0.5860(6)	0.9541(6)	7.07(31)
C8A	0.1470(6)	0.5957(7)	0.9631(8)	8.04(35)
C9A	0.0980(5)	0.5606(7)	0.8940(8)	8.18(36)
C10A	0.1129(4)	0.5154(6)	0.8112(6)	6.55(27)
C11A	0.2444(4)	0.6064(5)	0.6041(6)	5.73(24)
C12A	0.2374(5)	0.6733(5)	0.5353(7)	6.53(29)
C13A	0.1827(5)	0.6698(6)	0.4582(7)	7.06(28)
C14A	0.1388(4)	0.6037(6)	0.4499(6)	6.03(27)
C15A	0.1503(4)	0.5395(5)	0.5235(5)	4.60(21)
C16A	0.1058(4)	0.4648(5)	0.5208(5)	4.83(22)
C17A	0.0545(4)	0.4464(6)	0.4410(6)	5.86(25)
C18A	0.0152(4)	0.3754(6)	0.4464(7)	6.91(32)
C19A	0.0260(4)	0.3257(6)	0.5323(8)	6.91(31)
C20A	0.0789(4)	0.3468(5)	0.6082(6)	5.90(26)
Cl1	0.5658(1)	0.2070(2)	0.3603(2)	7.34(8)
O11	0.6312(4)	0.2032(9)	0.4038(7)	14.50(47)
O12	0.5485(6)	0.1386(8)	0.3037(9)	18.07(56)
O13	0.5306(5)	0.2158(8)	0.4350(9)	17.09(56)
O14	0.5635(8)	0.2796(9)	0.3064(10)	21.80(79)
NiB	0.29086(5)	0.10175(6)	0.82591(6)	4.32(2)
N1B	0.2954(3)	–0.0328(4)	0.8273(4)	5.64(20)
N2B	0.3697(3)	0.0804(4)	0.9414(4)	4.76(19)
N3B	0.3454(3)	0.1141(4)	0.7171(4)	5.16(19)
N4B	0.2178(3)	0.1117(4)	0.7010(4)	5.16(20)
N5B	0.2270(3)	0.1074(5)	0.9243(5)	5.97(21)
N6B	0.2415(3)	0.1209(4)	1.0098(5)	4.73(19)
N7B	0.2536(3)	0.1350(4)	1.0962(5)	5.46(21)
C1B	0.2559(5)	–0.0849(6)	0.7615(6)	7.05(29)
C2B	0.2682(6)	–0.1737(7)	0.7612(8)	8.03(37)
C3B	0.3213(7)	–0.2087(7)	0.8299(9)	8.88(40)
C4B	0.3598(5)	–0.1535(6)	0.8954(7)	7.46(32)
C5B	0.3448(4)	–0.0667(5)	0.8940(6)	5.49(24)
C6B	0.3823(4)	–0.0031(6)	0.9635(5)	5.17(21)
C7B	0.4292(4)	–0.0265(6)	1.0489(6)	6.49(29)
C8B	0.4628(4)	0.0380(7)	1.1068(6)	6.47(28)
C9B	0.4507(4)	0.1227(7)	1.0821(6)	6.41(30)
C10B	0.4019(4)	0.1409(6)	0.9967(6)	5.80(24)
C11B	0.4108(5)	0.1169(6)	0.7328(6)	6.78(32)
C12B	0.4462(5)	0.1314(6)	0.6569(8)	8.02(34)
C13B	0.4087(7)	0.1425(6)	0.5629(9)	8.37(39)
C14B	0.3412(6)	0.1419(6)	0.5453(6)	7.25(31)
C15B	0.3107(4)	0.1273(5)	0.6260(5)	5.25(22)
C16B	0.2385(5)	0.1273(5)	0.6160(5)	5.66(26)
C17B	0.1967(6)	0.1411(6)	0.5277(6)	6.82(30)
C18B	0.1319(6)	0.1386(7)	0.5242(7)	7.77(39)
C19B	0.1072(5)	0.1221(6)	0.6084(9)	8.21(36)
C20B	0.1545(5)	0.1081(6)	0.7012(7)	6.90(33)
C12	0.9513(2)	0.1451(2)	0.3196(2)	8.59(9)
O21	0.8919(6)	0.1679(13)	0.3041(10)	22.20(84)
O22	0.9502(8)	0.0674(8)	0.2722(8)	17.22(54)
O23	0.9726(5)	0.1383(9)	0.4215(6)	14.69(47)
O24	0.9949(10)	0.1907(10)	0.2879(10)	25.42(88)

^{a} $B_{eq} = (8\pi^2/3)\sum_i\sum_j U_{ij}a_i^*a_j^*\cdot\mathbf{a}_i\mathbf{a}_j$.

(16) Main, P.; Fiske, L.; Hull, S. E.; Lessinger, L.; Germain, G.; Declercq, J. P.; Woolfson, M. M., MULTAN 84, A System of Computer Programs for Crystal Structure Determination from X-ray Diffraction Data. Universities of York and Louvain, 1988.
(17) Sheldrick, G. M. SHELX 76, Program for Crystal Structure Determination. University of Cambridge, England, 1976.
(18) *International Tables for X-ray Crystallography*; Kynoch: Birmingham, England, 1974; Vol. IV, p 99.

Table 3. Fractional Atomic Coordinates and Equivalent Thermal Parameters for {[Ni(bipy)$_2$N$_3$](OF$_6$)}$_2$ (**2**)

atom	*x*	*y*	*z*	B_{eq},[a] Å^2
NiA	0.28570(5)	0.39110(6)	0.33162(6)	4.03(3)
N1A	0.2077(4)	0.3827(4)	0.2201(4)	5.08(21)
N2A	0.3303(4)	0.3864(4)	0.2115(4)	5.19(20)
N3A	0.2903(3)	0.5228(4)	0.3344(5)	5.32(20)
N4A	0.3661(3)	0.4115(5)	0.4370(4)	4.66(19)
N5A	0.2943(4)	0.2586(5)	0.3387(5)	5.15(20)
N6A	0.2504(4)	0.2127(5)	0.3133(4)	4.10(18)
N7A	0.2081(4)	0.1658(4)	0.2926(4)	5.01(20)
C1A	0.1467(5)	0.3817(6)	0.2325(7)	6.61(34)
C2A	0.0958(6)	0.3734(8)	0.1568(11)	8.65(47)
C3A	0.1112(7)	0.3665(8)	0.0623(11)	10.00(50)
C4A	0.1738(7)	0.3644(7)	0.0473(7)	8.23(42)
C5A	0.2243(5)	0.3728(5)	0.1292(6)	5.43(28)
C6A	0.2912(5)	0.3751(5)	0.1249(5)	5.33(26)
C7A	0.3148(8)	0.3658(7)	0.0376(7)	8.36(44)
C8A	0.3782(10)	0.3666(8)	0.0404(9)	10.63(56)
C9A	0.4224(7)	0.3727(7)	0.1304(9)	9.09(44)
C10A	0.3938(5)	0.3845(7)	0.2154(7)	7.13(34)
C11A	0.2516(5)	0.5753(6)	0.2735(7)	6.16(29)
C12A	0.2630(6)	0.6630(7)	0.2703(8)	7.81(40)
C13A	0.3177(7)	0.6933(7)	0.3332(10)	8.82(40)
C14A	0.3560(5)	0.6398(7)	0.3987(9)	7.41(37)
C15A	0.3406(4)	0.5556(6)	0.3977(6)	4.79(23)
C16A	0.3787(4)	0.4922(6)	0.4611(5)	4.80(24)
C17A	0.4257(4)	0.5149(8)	0.5426(6)	6.89(31)
C18A	0.4591(4)	0.4501(9)	0.5955(6)	6.63(34)
C19A	0.4488(4)	0.3667(8)	0.5695(7)	6.49(33)
C20A	0.3992(4)	0.3490(6)	0.4883(6)	5.57(26)
PA	0.4556(1)	0.7843(2)	0.6502(2)	7.05(09)
F1A	0.4462(4)	0.7696(8)	0.7570(6)	15.60(45)
F2A	0.5285(3)	0.7960(5)	0.6918(6)	11.34(30)
F3A	0.4422(5)	0.8780(6)	0.6587(9)	16.39(49)
F4A	0.4738(5)	0.6892(5)	0.6383(7)	13.68(40)
F5A	0.3848(4)	0.7697(8)	0.6102(8)	17.20(49)
F6A	0.4679(6)	0.7967(8)	0.5450(6)	18.36(52)
NiB	0.21408(5)	0.05775(6)	0.20634(6)	4.03(3)
N1B	0.2090(3)	−0.0467(4)	0.1120(4)	4.53(18)
N2B	0.1281(3)	0.0798(4)	0.1156(4)	4.50(18)
N3B	0.1810(3)	−0.0123(4)	0.3152(4)	4.80(19)
N4B	0.2994(3)	0.0219(4)	0.2930(4)	4.68(19)
N5B	0.2607(4)	0.1305(5)	0.1103(4)	5.92(24)
N6B	0.2461(3)	0.1229(4)	0.0248(5)	5.13(19)
N7B	0.2286(4)	0.1157(5)	−0.0601(5)	6.53(25)
C1B	0.2525(4)	−0.1105(6)	0.1184(6)	5.57(26)
C2B	0.2446(5)	−0.1778(6)	0.0527(8)	6.83(31)
C3B	0.1897(6)	−0.1769(7)	−0.0223(7)	7.66(39)
C4B	0.1462(5)	−0.1112(6)	−0.0304(6)	6.08(27)
C5B	0.1578(4)	−0.0461(5)	0.0394(5)	4.76(24)
C6B	0.1156(4)	0.0275(5)	0.0366(5)	4.53(21)
C7B	0.0647(4)	0.0432(6)	−0.0413(6)	5.91(30)
C8B	0.0272(5)	0.1140(7)	−0.0376(8)	6.68(31)
C9B	0.0389(4)	0.1670(6)	0.0428(8)	6.30(32)
C10B	0.0899(4)	0.1468(6)	0.1188(6)	5.71(26)
C11B	0.1204(5)	−0.0185(6)	0.3259(6)	6.40(29)
C12B	0.1011(5)	−0.0593(7)	0.4061(7)	7.22(31)
C13B	0.1512(6)	−0.0956(7)	0.4755(8)	8.13(37)
C14B	0.2135(5)	−0.0869(6)	0.4660(6)	6.81(32)
C15B	0.2279(4)	−0.0449(5)	0.3844(5)	4.93(23)
C16B	0.2942(4)	−0.0312(5)	0.3692(6)	4.80(24)
C17B	0.3467(5)	−0.0680(6)	0.4264(7)	6.46(30)
C18B	0.4072(5)	−0.0472(8)	0.4073(8)	7.58(40)
C19B	0.4143(4)	0.0094(7)	0.3331(7)	6.82(31)
C20B	0.3572(4)	0.0427(6)	0.2770(6)	5.70(27)
PB	0.0439(1)	0.6634(2)	0.1917(2)	7.94(10)
F1B	0.1104(3)	0.6228(6)	0.2088(6)	12.51(34)
F2B	0.0608(6)	0.7179(6)	0.2844(6)	15.39(44)
F3B	0.0669(5)	0.7274(8)	0.1217(7)	17.58(47)
F4B	−0.0247(4)	0.7002(8)	0.1718(6)	15.80(42)
F5B	0.0212(4)	0.5941(6)	0.2597(6)	13.45(39)
F6B	0.0260(4)	0.6013(9)	0.0990(6)	16.19(49)

[a] $B_{eq} = (8\pi^2/3)\sum_i\sum_j U_{ij}a_i^*a_j^*\cdot\mathbf{a}_i\mathbf{a}_j$.

(6), 2.085(6), 2.089(6), and 2.059(6) Å for **1** and 2.065(6), 2.061-(7), 2.080(7), and 2.071(6) Å for **2**] and the extreme nitrogens of the two azido ligands [NiA–N5A, –N7B^{ii}: 2.086(7) and 2.123-

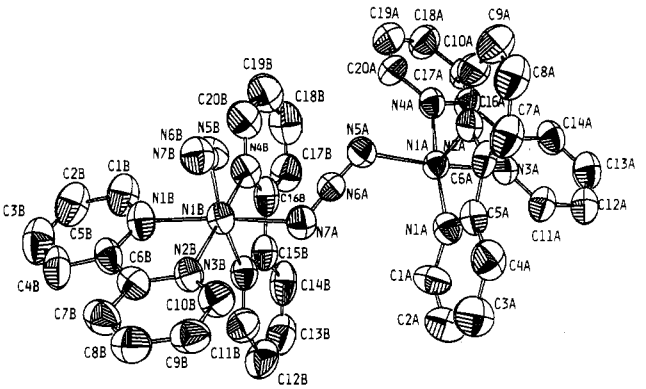

Figure 1. ORTEP view of the {[Ni(bipy)$_2$(N$_3$)]$_2$}$^{2+}$ entities which stack to generate the *cis*-azido Ni(II) chains, together with the atom labeling.

(7) Å for **1** and 2.100(7) and 2.093(8) Å for **2**; ii = x,$^1/_2 - y$, $z - ^1/_2$)] are in an octahedral *cis* arrangement. To our knowledge, this is the first nickel–azido chain structure with such an arrangement. Since the asymmetric unit contains two different nickel coordination polyhedra there are also two different end-to-end azido bridges, each one of them being asymmetrical [Ni–N–N angles being 123.7(6) and 120.1(6)° and 126.6(6) and 121.3(5)° for the perchlorate compound and 122.6(6) and 122.6-(6)° and 120.6(6) and 127.4(6)° for the hexafluorophosphate compound]. The distortion of the octahedral geometries has been evaluated using the Muetterties and Guggenberger description[19] to give Δ values near 0.06 for both compounds (supplementary material), which indicates a slight distortion from the ideal topology.

In Figure 3, the chain structures of **1** and **2** can be seen from the propagation axis viewpoint. The significant influence of the size of the different counterion in the resulting final structure can be observed. The hexafluorophosphate ions, which are larger than the perchlorate ones, compress the chain, normally in the direction of propagation, giving rise to variations in both torsion and bridging angles of structure **2**, in comparison with **1**. This fact will reflect significant variations in the magnetic properties of both compounds.

The azide ligands, having the angles N5A–N6A–N7A = 177.4-(7)° and N5B–N6B–N7B = 177.5(8)° for **1** and N5A–N6A–N7A = 176.8(7)° and N5B–N6B–N7B = 177.0(9)° for **2**, are also linear. The Ni–N–N–N–Ni torsion angles are 46.1 and 41.1° and 45.1 and 42.0° for compounds **1** and **2**, respectively.

In both complexes the bipy ligands may be considered as rigid and quasi-planar. The average C–C and C–N bond distances in the pyridine rings of this ligand are 1.42(1) and 1.35(1) Å, and 1.41(1) and 1.35(1) Å for compounds **1** and **2**, respectively. These values are in good agreement with those currently given in the literature for this ligand.[13-15]

Infrared and Diffuse Reflectance Spectroscopies. Infrared spectra of both complexes show the characteristic bands of the bipy ligand,[20] but these bands are shifted to higher frequencies and unfolded by coordinating with the metal. However, the more interesting bands are those associated with the azido groups. The IR spectra of both compounds **1** and **2** show the $\nu_{as}(N_3)$ band splitting at several peaks of different intensities: 2060, 2040, and 2010 cm^{-1}. It suggests a coordination of the azide bridging group at both extremes, in good accordance with the structural results. Very weak bands appear at 1345 cm^{-1} in both compounds, corresponding to the $\nu_s(N_3)$ vibration mode. This mode is inactive in dinuclear structures with end-to-end azido bridges, which possess high symmetry.[21] Its presence in the studied compounds

(19) Muetterties, E. L.; Guggenberger, L. J. *J. Am. Chem. Soc.* **1974**, *96*, 1748.
(20) McWhinnie, W. R.; Miller, J. D. *Adv. Inorg. Chem. Radiat.* **1969**, *12*, 135.
(21) Nelson, J.; Nelson, S. M. *J. Chem. Soc. A* **1969**, 1597.

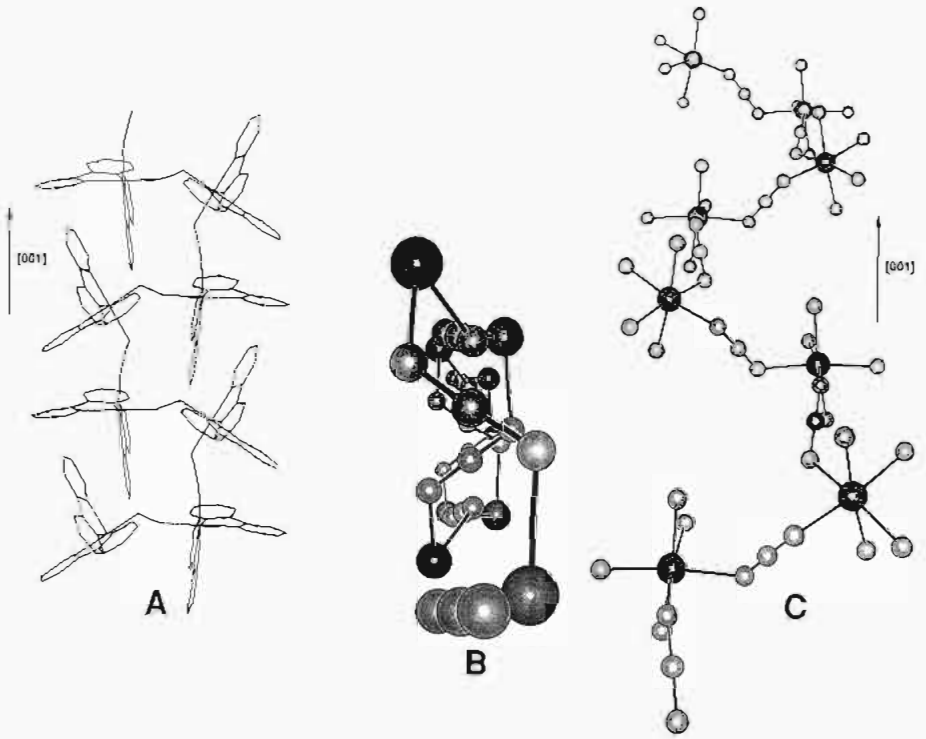

Figure 2. Different perspective views of the chains propagation along the [001] direction (A and C) and from the propagation axis viewpoint (B).

Table 4. Selected Bond Distances (Å) and Angles (deg) for the $[Ni(bipy)_2N_3]Y$ (Y = ClO_4 (**1**), PF_6 (**2**)) Compounds[a]

	1	2		1	2
NiA–N1A	2.065(6)	2.065(6)	NiB–N1B	2.088(6)	2.099(6)
NiA–N2A	2.085(6)	2.061(7)	NiB–N2B	2.076(6)	2.057(6)
NiA–N3A	2.089(6)	2.080(7)	NiB–N3B	2.077(7)	2.094(7)
NiA–N4A	2.059(6)	2.071(6)	NiB–N4B	2.069(6)	2.070(6)
NiA–N5A	2.086(7)	2.100(7)	NiB–N5B	2.095(8)	2.131(8)
NiA–N7B^{ii}	2.123(7)	2.093(8)	NiB–N7A	2.129(7)	2.103(7)
N1A–NiA–N2A	78.6(2)	78.8(2)	N1B–NiB–N2B	78.8(2)	78.8(2)
N1A–NiA–N3A	97.1(2)	96.1(3)	N1B–NiB–N3B	93.9(3)	93.0(2)
N1A–NiA–N4A	174.7(2)	174.0(3)	N1B–NiB–N4B	96.1(3)	95.4(3)
N1A–NiA–N5A	89.6(3)	91.3(3)	N1B–NiB–N5B	94.0(3)	90.5(2)
N2A–NiA–N3A	93.4(2)	91.4(3)	N2B–NiB–N3B	96.6(3)	99.4(3)
N2A–NiA–N4A	98.9(3)	98.3(3)	N2B–NiB–N4B	172.7(3)	173.8(3)
		Azides			
N5A–N6A	1.181(9)	1.182(10)	N5B–N6B	1.183(10)	1.183(9)
N6A–N7A	1.169(9)	1.160(10)	N6B–N7B	1.197(9)	1.181(9)
NiA–N5A–N6A	123.7(6)	122.6(6)	NiB–N5B–N6B	126.6(6)	120.6(6)
N6A–N7A–NiB	120.1(6)	122.6(6)	N6B–N7B–NiA^{ii}	121.3(5)	127.4(6)
N5A–N6A–N7A	177.4(7)	176.8(7)	N5B–N6B–N7B	177.5(8)	177.0(9)

[a] ii = $x, 1/2 - y, z - 1/2$.

indicates an asymmetry of the bridging groups in good accordance with the observed chain structures. The deformation mode of the azido ligand is obscured by a band corresponding to the perchlorate ion in compound **1**, while it appears at 615 cm^{-1} in compound **2**. The characteristic bands of the perchlorate ion appear at 1090 (ν_3) and 625 cm^{-1} (ν_4), and those corresponding to the hexafluorophosphate are located without splitting at 850 and 550 cm^{-1}, in both cases indicating that these groups act only as counterions.

The reflectance spectra of compounds **1** and **2** are very similar, showing the three characteristic bands of the Ni(II) complexes in a slightly distorted octahedral environment.[22] The bands are localized at 10 000, 14 800, and 26 000 cm^{-1} [$^3A_{2g} \rightarrow {}^3T_{2g}$ (ν_1), $^3T_{1g}$ (F) (ν_2), and $^3T_{1g}$ (P) (ν_3), respectively]. An extra weak band appearing at 12 400 cm^{-1} has been attributed to the forbidden spin transition $^3A_{2g} \rightarrow {}^1E_g$ (ν_4). The appearance of this band allows the calculation of the Racah parameter to be $C = 3192$ cm^{-1}. The nephelauxetic parameter is 0.79, in the range obtained for octahedral Ni(II) compounds.[22]

Magnetic Measurements. The thermal variations of magnetic susceptibility of both compounds are shown together in Figure 4. The molar susceptibility value (3.24×10^{-3} cm^3 mol^{-1} for **1** and 3.48×10^{-3} cm^3 mol^{-1} for **2** at room temperature) increases with decreasing temperature, reaching a maximum of 6.21×10^{-3} cm^3 mol^{-1} at 69 K and 9.41×10^{-3} cm^3 mol^{-1} at 39 K for **1** and **2**, respectively, and then rapidly decreases. The $\chi_m T$ value decreases from 0.93 cm^3 K mol^{-1} (300 K) to 0.02 cm^3 K mol^{-1} (4.2 K) for perchlorate and from 0.98 cm^3 K mol^{-1} (300 K) to 0.05 cm^3 K mol^{-1} (4.2 K) for the hexafluorophosphate chains, tending to zero. Both the continuous decrease in the $\chi_m T$ value and the maximum observed in the thermal variation of the molar susceptibility clearly indicate the existence of strong antiferromagnetic intrachain interactions in the perchlorate (**1**) and hexafluorophosphate (**2**) compounds. Curie–Weiss behavior cannot be observed even at room temperature.

(22) Lever, A. B. P. *Inorganic Electronic Spectroscopy*, 2nd ed.; Elsevier: Amsterdam, 1986.

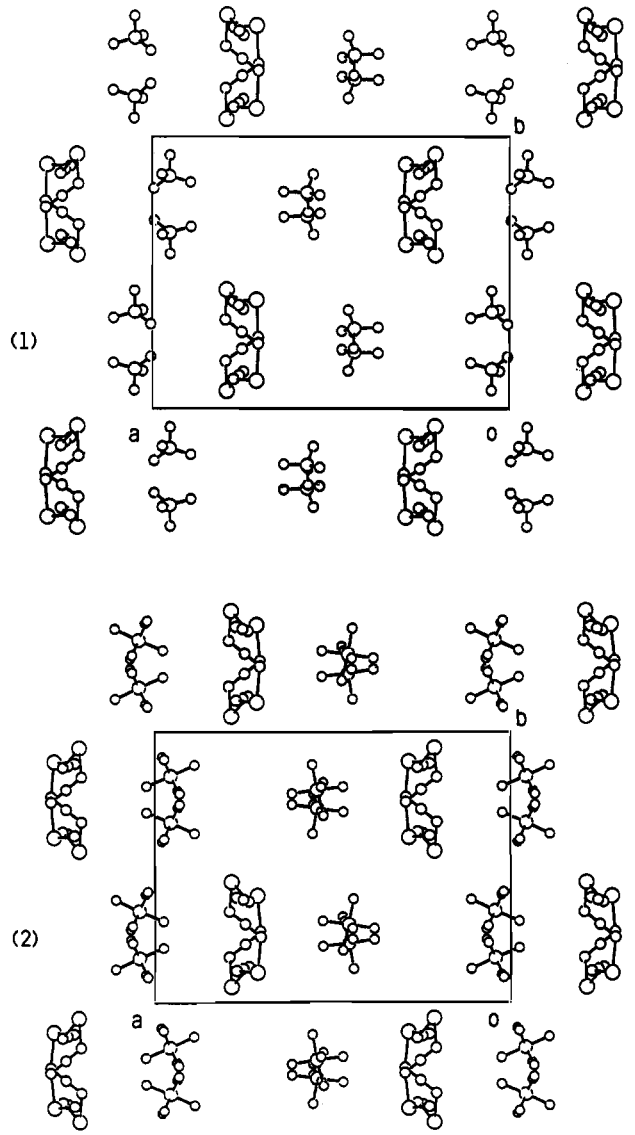

Figure 3. Comparative view of the unit cells of both the perchlorate (**1**) and hexafluorophosphate (**2**) chains showing the influence of the counterion on the final structure.

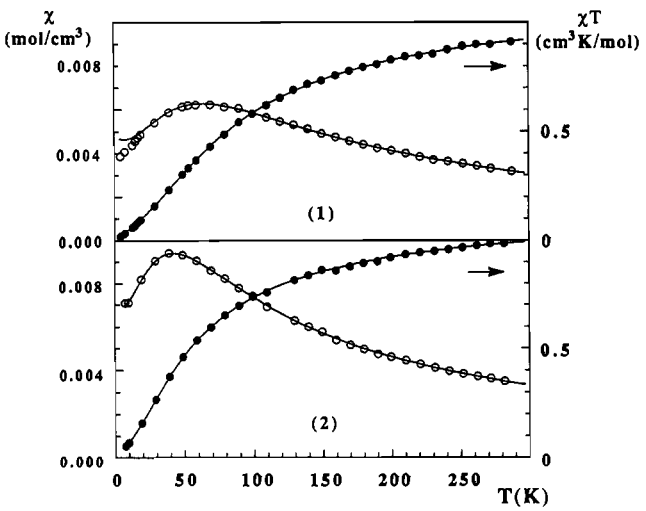

Figure 4. Thermal variations of the magnetic susceptibility (χ) and χT product for [Ni(bipy)$_2$(N_3)](ClO_4) (**1**) and [Ni(bipy)$_2$(N_3)](PF_6) (**2**).

The single-ion ground term of Ni(II) in a pseudooctahedral environment is $^3A_2$ and hence has no orbital momentum of the first order. The more general spin Hamiltonian to describe the magnetic properties of isotropic Ni(II) chains is as follows taking into consideration only the single-ion terms and the interactions between the nearest-neighbor centers:

$$H = \sum_i (\beta \hat{S}_i \cdot g_i \vec{H} - J \hat{S}_i \cdot S_{i+1})$$

Here the first term represents the Zeeman perturbation, and the second the isotropic exchange. The terms corresponding to the anisotropic exchange and antisymmetric exchange have not been considered because these effects are only relevant at very low temperatures (near 1 K) and besides they are much less important in comparison with a large exchange coupling.

There is no exact analytical expression for the temperature dependence of the susceptibility of infinite isotropic Heisenberg chains. Nevertheless, there exist numerical calculations that approximately characterize the Heisenberg behavior, especially in the 1D case.[23,24] For S = 1 the characteristic expressions are as follows:[25]

$$\frac{kT(\chi_{max})}{|J|} \approx 1.35 \quad (1)$$

$$\frac{\chi_{max}|J|}{Ng^2\beta^2} \approx 0.176 \quad (2)$$

$$\frac{\chi_{max}T(\chi_{max})}{g^2} \approx 0.089 \quad (3)$$

By substitution of the experimental data $T(\chi_{max})$ [temperature corresponding to the maximum in susceptibility] = 69 K for **1** (39 K for **2**), χ_{max} = 0.0062 cm^3 mol^{-1} for **1** (0.0094 cm^3 mol^{-1} for **2**), and considering g = 2.15 (usual for octahedral Ni(II) complexes), we obtain J = 51.4 K (35.6 cm^{-1}) in (1) and J = 49.2 K (34.2 cm^{-1}) in (2) for perchlorate [J = 31.8 K (22 cm^{-1}) in (1) and J = 31.0 K (21.4 cm^{-1}) in (2) for hexafluorophosphate]. In the studied compounds **1** and **2**, according to the structural results, two different azido bridges indicate that two different J values are to be expected; however, they must be very similar. These results seem to indicate that the observed magnetic behavior can be interpreted as that corresponding to isotropic 1D antiferromagnetic systems.

In the case of these isotropic 1D systems with S = 1, the temperature dependence of the susceptibility extrapolated from calculations performed on ring chains of increasing length has been given by Weng.[26] To reproduce Weng's results, Kahn[27] introduced the following empirical function:

$$\chi_{chain} = \frac{N\beta^2g^2}{kT}\left[\frac{2 + 0.0194X + 0.777X^2}{3 + 4.346X + 3.232X^2 + 5.834X^3}\right] \quad (4)$$

$$X = |J|/kT$$

It is only valid for an antiferromagnetic coupling, assuming the nickel ion is magnetically isotropic.

Using this expression, excellent agreements between the observed and calculated χ_m values (solid lines in Figure 4) have been obtained. The magnetic exchange values are J = –48 K (–33.0 cm^{-1}) for compound **1** and J = –32 K (–22.4 cm^{-1}) for compound **2** with a g value of 2.15 in both cases. The fit is only possible up to a certain temperature value. This is because zero-field splitting and the Haldane gap have not been considered in eq 4. The agreement factors, defined as SE = $[\Phi/(n - K)]^{1/2}$, where n is the number of data points, K is the number of adjustable

(23) Blöte, H. W. *Am. J. Phys.* **1964**, *32*, 343.
(24) De Neef, T.; Kuipers, A. J. M.; Kopinga, K. *J. Phys.* **1974**, *A7*, L171.
(25) Carlin, R. L. *Magnetochemistry*; Springer-Verlag: Berlin, 1986.
(26) Weng, C. Y. Ph.D. Thesis, Carnegie Institute of Technology, 1968.
(27) Meyer, A.; Gleizes, A.; Girerd, J. J.; Verdaguer, M.; Kahn, O. *Inorg. Chem.* **1982**, *21*, 1729.

Table 5. Structural and Magnetic Parameters for the Known 1D Ni(II)–Azido Systems[a]

compd, confign	bond length Ni–N(azido), Å		bond angle Ni–N–N, deg		torsion angle Ni–N–Ni, deg		square gap (Δ^2)	J, cm^{-1}	ref
$[Ni(cyclam)N_3]ClO_4$,	2.165		128.2		13.1		0.133	−39.2	12
trans	2.172		140.7						
$[Ni(tmd)N_3]ClO_4$,	2.122		120.9		0		0.338	−70.0	31
trans	2.122		120.9						
$[Ni(232\text{-tet})N_3]ClO_4$,	2.151		124.1		37.6		0.130	−27.7	32
trans	2.156		134.6						
$[Ni(323\text{-tet})N_3]ClO_4$,	2.181		119.8		10.7		0.207	−60.1	32
trans	2.129		135.8						
$[Ni(bipy)_2N_3]ClO_4$,	2.086	2.095	120.1	121.3	46.1	41.1	0.705	−33.0	this work
cis	2.123	2.129	123.7	126.6					
$[Ni(bipy)_2N_3]PF_6$,	2.100	2.131	120.6	122.6	45.1	42.0	0.620	−22.4	this work
cis	2.093	2.103	122.6	127.4					

[a] Abbreviations: cyclam = 1,4,8,11-tetraazacyclotetradecane; tmd = 1,3-diaminopropane; 232-tet = *N,N'*-bis(2-aminoethyl)-1,3-propanediamine; 323-tet = *N,N'*-bis(3-aminopropyl)-1,2-ethanediamine; bipy = 2,2'-bipyridine.

parameters in (2), and $\Phi = \sum[\chi_m T_{obs} - \chi_m T_{calc}]^2$ is the sum of squares of the residuals, are equal to 8×10^{-4} and 7.8×10^{-4} for compounds **1** and **2**, respectively. The obtained J values clearly indicate the high efficiency of single end-to-end azido bridges in transmitting antiferromagnetic interactions in good accordance with other Ni(II) chains containing oxalate[28] ($J = -24$ cm^{-1}), nitrite[27] ($J = -33$ cm^{-1}), or halogen[29,30] ($J = -18$ to -35 cm^{-1}) bridging ligands.

Finally, it must be noted that, at low temperatures, the susceptibility data for these two chains do not show the characteristic exponential drop-off toward zero, but they remain high and continue to follow the predictions for the susceptibility of the gapless antiferromagnetic chain. Such behavior has never been seen before, which make the obtained chains remarkable.

Magnetostructural Study and MO Calculations. To date, not a great many Ni(II)–azido chains have been characterized, which makes it difficult to propose clearly magnetostructural correlations of these kinds of compounds. Table 5 compiles the structural and magnetic data available for the known chains[12,31,32] with a *trans* arrangement of the azido ligands and the data corresponding to the title complexes with a *cis* arrangement. It can be observed that the bond distances are very similar in all the reported complexes and they are obviously not of great significance in determining the strength of the magnetic interactions. As the azido ion is practically linear, the magnitude of the antiferromagnetic interaction will depend on the Ni–N–N and Ni–N_3–Ni angles. These factors will play the most significant role in the superexchange interaction between the nickel atoms. Extended Hückel molecular orbital (EHMO) calculations have been performed for the *trans*-nitrito[27] and *trans*-azido[32] 1D chains. In both cases, the antiferromagnetic component of J is a function[33] of the sum of the square of the gaps between the xy and z^2 pairs of molecular orbitals: $\sum\Delta^2 = \Delta^2(xy) + \Delta^2(z^2) = |E\Phi xy - E\Phi xy|^2 + |E\Phi z^2 - E\Phi z^2|^2$. In a *trans* chain with the d_{z^2} orbitals placed in the chain direction, the xy orbital is perpendicular and the overlap with the bridge is negligible. In these kinds of nickel chains the gap between the symmetric and antisymmetric d_{z^2} combinations, and therefore the antiferromagnetic J values, has been observed to be very sensitive to small variations in Ni–N–N angles and Ni–N_3–Ni torsion angles. A maximum in the antiferromagnetic coupling for the system is found at a Ni–N–N angle of 108° and a Ni–N_3–Ni torsion angle of 0°.[28]

In the *cis*-azido chains, $\Delta^2(xy)$ is not zero and must obviously be considered in the study. In this work, MO extended Hückel calculations have been performed by means of the CACAO[34] program. A scheme involving three nickel units with a cis arrangement has been considered for the study:

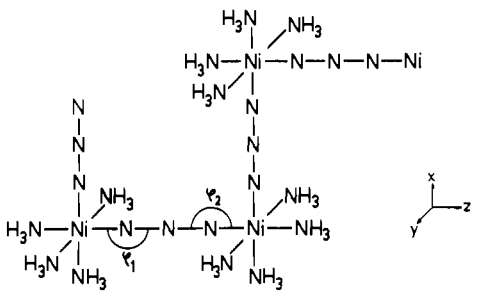

General calculations have been done by varying the bridging (φ_1, φ_2) and torsion Ni–N_3–Ni angles (Ni–N distances have been assimilated to Ni–NH_3 = 2.10 Å and N1–N2 equal to N2–N3 = 1.17 Å). The standard atomic parameters of the program were used. A set of 14×14 $\sum\Delta^2[\Delta^2(z^2) + \Delta^2(xy)]$ values calculated at φ_1 and φ_2 in the 95–160° range, varying every 5° and maintaining the torsion angle Ni–N_3–Ni equal to 0°, have been performed. The results are shown in Figure 5. As can be observed, a maximum for antiferromagnetic coupling appears for $\varphi_1 = \varphi_2 = 110°$; it rapidly decreases with larger bridging angles. The average bridging angles are 122.95 and 123.32° for compounds **1** and **2**, respectively. The larger angle for compound **2** is attributed to the smaller antiferromagnetic coupling observed in it, in good accordance with the results of the EHMO calculations. Nevertheless, the differences should not be as significant as the ones observed.

The effect of the Ni–N_3–Ni torsion angle has been parametrized by means of a set of 14×11 values of $\sum\Delta^2[\Delta^2(z^2) + \Delta^2(xy)]$ for a symmetric variation of $\varphi_1 = \varphi_2$ between 95–160° and torsions between 0–50°, varying every 5° in both cases. The result (shown in Figure 5) indicates that for all the bridging angle values the maximum antiferromagnetic coupling can be expected at a torsion value of 0°, decreasing for larger values of torsion. For the title compounds the average Ni–N_3–Ni torsion angles are very similar with a value around 44°. In this sense, their antiferromagnetism is less favorable than that corresponding to a torsion angle near to 0. The second effect is lower in magnitude with respect to the bridging angle.

Concluding Remarks

A synthetic method has been successfully employed to obtain one-dimensional Ni(II) systems with azido bridging ions in a *cis*

(28) Kralingen, C. G. V.; Van Ouijen, J. A. C.; Reedjik, J. *Transition Met. Chem. (Weinheim, Ger.)* **1978**, *3*, 90.
(29) Brener, R.; Ehrenfreund, E.; Shechter, H.; Makovsky, J. *J. Phys. Chem. Solids* **1977**, *38*, 1023.
(30) Witteveen, H. T.; Vann Veen, J. A. R. *J. Phys. Chem. Solids* **1974**, *35*, 337.
(31) Gadet, V.; Verdaguer, M.; Renard, J. P.; Ribas, J.; Monfort, M.; Diaz, C.; Solans, X.; Landee, C. P.; Jamet, J. P.; Dworkin, A. *J. Am. Chem. Soc.*, in press.
(32) Escuer, A.; Vicente, R.; Ribas, J.; Salah El Fallah, M.; Solans, X.; Font-Bardia, M. Submitted for publication in *Inorg. Chem.*
(33) Jeffrey Hay, P.; Thibeault, J. C.; Hoffmann, R. *J. Am. Chem. Soc.* **1975**, *97*, 4884.
(34) Mealli, C.; Proserpio, D. M. CACAO program (Computed Aided Composition of Atomic Orbitals). *J. Chem. Educ.* **1990**, *67*, 399.

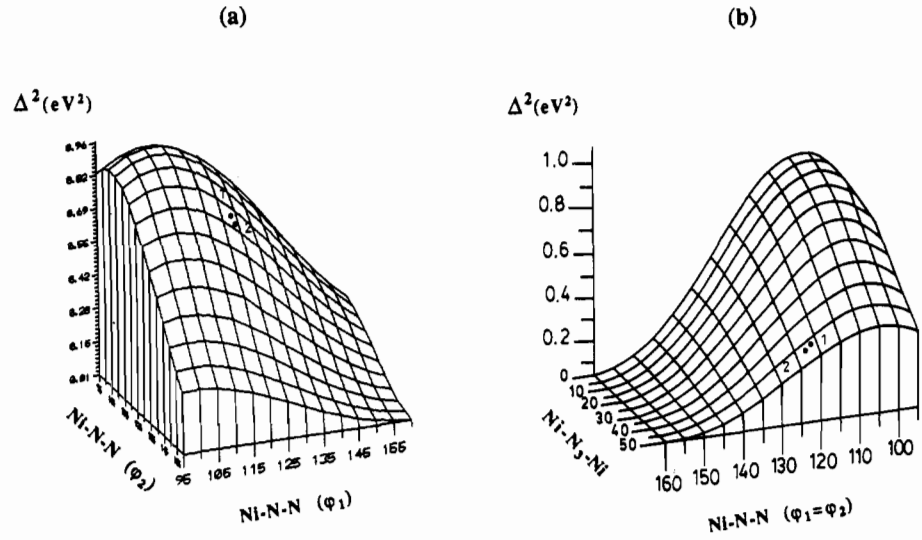

Figure 5. (a) Variation of the square gap (Δ^2) as a function of the bridging angles maintaining torsions equal to 0. (b) Variation of Δ^2 as a function of the torsion and bridging angles with $\varphi_1 = \varphi_2$.

arrangement. Although the compounds are isostructural, the influence of the two different counterions cause variations in both the bridging and torsion angles, giving rise to significant variations in the magnetic properties. Contrary to the observed in the few reported Ni(II) chains, the predictions of Haldane for antiferromagnetic integer-spin magnetic chains are not followed by the title chains, but they behave as gapless antiferromagnetic ones. This makes remarkable these two compounds. Extended Hückel MO orbital calculations have been used to propose a simple model correlating magnetic and structural parameters in these kinds of 1D nickel compounds. The bridging Ni–N–N angle has been shown to be the most significant parameter correlating the magnitude of antiferromagnetism. Following these results, the minor value of the bridging angle corresponding to the perchlorate compound must be associated with larger antiferromagnetic interactions, as does occur. However, the influence of the Ni–N_3–Ni torsion angle must also be considered, although to a minor degree. Finally, it would be desirable to obtain new *cis*-azido–Ni(II) chains, with their corresponding magnetic characterization, to corroborate the observed significant factors correlating the superexchange mechanism.

Acknowledgment. This work has been carried out with the financial support of the Universidad del Pais Vasco/Euskal Herriko Unibertsitatea (UPV 130.310.EB017/92) and the Ministerio de Educación y Ciencia (DGICYT PB90-0549 Grant), which we gratefully acknowledge.

Supplementary Material Available: Tables giving details of structural determinations, anisotropic thermal parameters, bond distances and angles, and distortions of the coordination polyhedra (35 pages). Ordering information is given on any current masthead page.